



## Research Article

# Global assessment of historical changes in extreme fire weather: Insight from CMIP6 ensembles and implications for probabilistic attribution to global warming

Zhongwei Liu<sup>a,b,\*</sup>, Jonathan M. Eden<sup>a</sup>, Bastien Dieppois<sup>a</sup>, Igor Drobyshev<sup>c,d</sup>, Folmer Krikken<sup>e</sup>, Matthew Blackett<sup>f</sup>

<sup>a</sup> Centre for Agroecology, Water and Resilience (CAWR), Coventry University, UK

<sup>b</sup> National Centre for Earth Observation, University of Leicester, UK

<sup>c</sup> Southern Swedish Forest Research Centre, Swedish University of Agricultural Sciences, Alnarp, Sweden

<sup>d</sup> Institut de recherche sur les forêts, Chaire de recherche du Canada en aménagement forestier durable, Université du Québec en Abitibi-Témiscamingue (UQAT), Canada

<sup>e</sup> Royal Netherlands Meteorological Institute (KNMI), Research and Development of Weather and Climate models, De Bilt, Utrecht, the Netherlands

<sup>f</sup> School of The Environment, Coventry University, UK

## ARTICLE INFO

Editor: Dr. Alan Haywood

## Keywords:

Wildfires

Fire weather

CMIP6 multi-model large ensembles

Climate change attribution

Extreme value statistics

## ABSTRACT

In response to the occurrence of several large wildfire events across the world in recent years, the question of the extent to which climate change may be altering the meteorological conditions conducive to wildfires has become a hot topic of debate. Despite the development of detection and attribution methodologies for climate change impact assessment in the last decade, studies dedicated explicitly to wildfire, or otherwise extreme ‘fire weather’, are still relatively few. Here, for the first time, a global probabilistic framework is developed to examine the extent to which externally forced changes in historical global mean surface temperature anomalies (GMSTA) affected the intensity and duration of fire-conducive weather extremes, defined by the Fire Weather Index (FWI). We use six climate model large ensembles (>10 ensemble members) from the sixth phase of the Coupled Model Intercomparison Project (CMIP6), to extract the forced response of GMSTA. After evaluating the performances of these climate models in simulating fire weather extremes, we examine changes in the probability of fire weather extremes using extreme value distributions, fitted with annual maxima in both FWI intensity and duration, and scaled to externally forced GMSTA. Global probability ratio maps are used to quantify the influence of rising global temperatures on the changing frequency and duration of FWI extremes, and highlight the sensitivity of estimates of historical changes in extreme fire weather to the climate model ensemble chosen for the analysis. A multi-model synthesis accounting for performance of each model confirms an increasing trend in the probability and duration of extreme fire weather linked to externally forced changes in GMSTA, with the largest increases found in southern North America, south-eastern Europe and parts of Australia. The results of the selective synthesis differ from those obtained via a conventional multi-model averaging that does not account for model performance, thereby demonstrating the value added by model evaluation and selection in maximising the robustness of probabilistic attribution studies.

## 1. Introduction

The frequency and severity of large wildfire events have increased globally in recent years (World Meteorological Organization, 2021). Particularly destructive fires have fostered debate on how the role of climate change may have altered the weather conditions favourable to

wildfires (Boer et al., 2020; Bowman et al., 2020; Ellis et al., 2022). Efforts to quantify the role of climate change in altering the frequency and magnitude of weather and climate phenomena, broadly termed, climate change attribution, have developed extensively during the last decade and form an important part of climate change impact assessment. However, attribution studies focused specifically on wildfire

\* Corresponding author at: Centre for Agroecology, Water and Resilience (CAWR), Coventry University, UK.

E-mail address: [zl341@leicester.ac.uk](mailto:zl341@leicester.ac.uk) (Z. Liu).

<https://doi.org/10.1016/j.gloplacha.2025.104822>

Received 24 May 2024; Received in revised form 24 March 2025; Accepted 4 April 2025

Available online 9 April 2025

0921-8181/© 2025 The Authors. Published by Elsevier B.V. This is an open access article under the CC BY license (<http://creativecommons.org/licenses/by/4.0/>).

events are rare in comparison to those focused on other, more widespread, extreme events, such as heatwaves, meteorological floods, and droughts.

The general scarcity of climate change impact assessment related to wildfire is surprising given that the link between wildfires and weather is well-established and widely used in operational fire management, e.g., through the reliance of forest management agencies on the Canadian Fire Weather Index System (Van Wagner, 1987) and the United States National Fire Danger Rating System (Deeming et al., 1977). The Atlas of Mortality and Economic Losses from Weather, Climate and Water Extremes (1970–2019) (World Meteorological Organization, 2021) categorises wildfires as part of the ‘climatological’ subgroup of hazards. Strictly speaking, however, wildfires are not meteorological events, distribution and properties of fuels, ignition patterns are controlled by climate variability and human land use patterns. These interactions make controls of fire activity more complex, and their relationship to weather and climate more obscure. With respect to attribution, the confidence and reliability of studies focused on specific events is limited by a poorer understanding of the occurrence mechanism of wildfires in comparison to other extremes (National Academies of Science, Engineering and Medicine, 2016). Additionally, estimates of climate change impact upon the future wildfire activity is associated with uncertainty relating to the choice of fire weather indicators (Liu et al., 2022a), and the climate models used in the analysis (Philip et al., 2020).

Research on the potential impact of climate change on extreme wildfires, particularly when framed in the context of attribution, remains scarce, and even more so on a global scale, with only a few global studies having examined changes affecting fire-prone weather, so called fire weather. For instance, according to Abatzoglou et al. (2019), 22 % of the world’s burnable land area is experiencing anthropogenically-induced increases in extreme fire weather indices by 2019, including much of the Mediterranean and Amazon. Jain et al. (2022) found trends in extreme fire weather across almost half of the global burnable area based on the reanalysis data from 1979 to 2020. Additionally, Liu et al. (2022a) showed that, across more than 40 % of the world’s fire-prone regions, extreme fire weather became at least four times more likely due to global temperature increases between 1980 and 2018. There is enormous potential for regional- and local-scale studies to support and test global-scale frameworks’ findings. Recent case studies have been undertaken in regions of Australia (Tett et al., 2018; Lewis et al., 2020; van Oldenborgh et al., 2021a), Canada (Kirchmeier-Young et al., 2017), Sweden (Krikken et al., 2021), Siberia (Liu et al., 2022b) and South Africa (Liu et al., 2023). The emergence of the *World Weather Attribution* initiative has provided a platform for the dissemination of rapid attribution analyses, often in the immediate aftermath of wildfire events (e.g., Barnes et al., 2023; Kimutai et al., 2024). Nevertheless, studies focused on the impact of climate change on wildfires, or otherwise extreme fire weather events, are rare in comparison to other weather and climate extremes.

While event-based regional studies are an important supplement to global analysis, the extent to which their results can be integrated is limited by a lack of consistency in the spatio-temporal definition of the event and the choice of methodology. In turn, this limits our ability to gauge changes in the frequency of fire-prone conditions and their impacts across the range of Earth’s biomes. In that sense, Liu et al. (2022a) provided clarity on the sensitivity of the findings of a global empirical probabilistic methodology in the definition of extreme fire weather. Such analysis of observational data is an important first step in event-based attribution studies (e.g., Liu et al., 2022b, 2023). In addition, similar methods are frequently applied to transient simulations from model ensembles (including those that contribute to the Coupled Model Intercomparison Project), either as an alternative to or to supplement results from attribution approaches that target fixed forcing runs (Philip et al., 2020).

The role of climate models is indeed vital to provide robust climate change impact assessment. Despite the widespread use of climate model

ensembles in climate change impact assessment, many attribution studies are based on a small number of models (Kirchmeier-Young et al., 2017; Kirchmeier-Young et al., 2019; Liu et al., 2022b), or otherwise perform no more than a cursory check of model output (Kirchmeier-Young et al., 2017). All climate models exhibit (potentially large) biases, particularly in the representation of extremes (e.g., Vautard et al., 2020). The capability of climate models to simulate statistics of extreme events that are comparable to the observed one has not always been given due attention, leading to uncertainties in the findings drawn from the analysis of simulations from different climate models. This set of circumstances introduces new questions about the suitability of the chosen climate model for assessment of climate change impact arising from a specific extreme event (Philip et al., 2020). As noted by Philip et al. (2020) in their documentation of recommended protocols for probabilistic attribution of extreme events, it is important to examine a series of climate models to understand the potential uncertainties and include a thorough model evaluation.

The fast-paced development of probabilistic extreme event attribution analysis during the last decade has been driven by the increased capacity for climate models to simulate large ensembles. Climate model large ensembles provide: (a) an opportunity to study multiple realizations and thus longer time series than what is possible with observations alone, which means that the detection and quantification of extreme thresholds and distributions should be more robust, (b) a homogeneous representation of climate, independent of the spatial and temporal distribution of the observational monitoring network, and (c) a better understanding of the role of externally forced trends (Deser et al., 2020). Notably, the use of large ensembles (defined here as >10 realizations of the same model) of coupled general circulation models enables smoothing the impact of internal variations and extraction of more robust externally forced signals, as well as for global mean surface temperatures, which is not possible with single-member ensembles (Milinski et al., 2020; Maher et al., 2021).

With a growing number of probabilistic attribution studies dedicated to wildfire, or extreme fire weather, across the globe, there is a clear need to identify and understand multiple sources of uncertainties. Here, we use established statistical methodologies applied to six large ensembles from the sixth phase of the Coupled Model Intercomparison Project (CMIP6) to assess changes in the probability of both the intensity and duration of extremes in the Canadian Fire Weather Index) using a Generalised Extreme Value (GEV) distribution, fitted with annual maxima and scaled to historical externally forced global mean surface temperature anomalies (GMSTA). In terms of the analysis of extremes in fire weather intensity, the current analysis builds on the empirical-statistical approach presented by Liu et al. (2022a). For the first time, we apply this approach to the output of multiple large ensembles from CMIP6 models. The extension of the same approach to quantify trends in the duration of extreme fire weather events also constitutes a novel application. We place particular emphasis on model evaluation in order to present the most robust possible multi-model assessment of historical changes in extreme fire weather, and to highlight the added value of an objective model selection step in attribution analysis.

The remainder of this paper is structured as follows. In Section 2, details of the CMIP6 data and methodology are presented, including the selection of a definition for global fire weather extremes. In Section 3, results of the changing likelihoods in extreme fire weather and a multi-model synthesis are presented. In Section 4, we conclude and make a set of recommendations for future probabilistic attribution of extreme fire weather episodes.

## 2. Methods and data

### 2.1. Defining fire weather extremes

Fire-climate studies have utilised a range of different indices and metrics to represent fire-conducive meteorological conditions. Such

indicators are typically defined by national organisations focused on disseminating information about fire danger. Examples include the McArthur Forest Fire Danger Index from the Centre for Australia Weather and Climate Research (McArthur, 1967) and the Keetch–Byram drought index from the US National Fire Danger Rating System (Deeming, 1972). The set of indices that form the Canadian Fire Weather Index System (CFWIS; Van Wagner, 1987) are particularly well known and, despite the system’s original development for Canadian pine forests, widely applied across the world, for instance as a key input for both the *European Forest Fire Information System* and the *Global Wildfire Information System* (Gallo et al., 2023). The system combines daily readings of temperature, precipitation, relative humidity, and wind speed to determine a range of fire danger indicators. These include fire fuel moisture-related indices (Fine Fuel Moisture Code, Drought Code, and Duff Moisture Code), as well as fire behavior indices (Initial Spread Index and Build-Up Index), which rely on different subsets of the four climate variables. These indicators collectively contribute to a numerical rating of overall fire danger, known as the Fire Weather Index (FWI) (Vitolo et al., 2020). CFWIS indicators have been used extensively to define fire-climate relationships, notably in the context of attribution (e.g., Du et al., 2021; Krikken et al., 2021; Barnes et al., 2023). The appropriateness of the indicator, whether from the CFWIS or an alternative system, is an important consideration and the choice has substantial dependence on circumstance and location (Liu et al., 2022a, 2022b). Here, FWI is selected as the most appropriate fire weather indicator for our analysis based on its widespread applicability and familiarity.

Choosing an appropriate set of spatio-temporal parameters by which to define weather or climate extremes is a crucial step in climate change impact assessment, since the findings and interpretation of the results both rely upon this definition. To this end, fire weather extremes are defined in terms of the danger posed irrespective of the meteorological drivers (Philip et al., 2020; Krikken et al., 2021; van Oldenborgh et al., 2021b). Specifically, fire weather extremes are defined in two ways:

- (i) Extremes in fire weather intensity are defined by the annual maxima in 7-day averaged FWI (FWIx7day). The choice of 7-days for averaging is consistent with previous efforts to attribute FWI extremes (e.g., Krikken et al., 2021; Liu et al., 2022b, 2023).
- (ii) Extremes in fire weather duration are defined by the annual maxima in the number of consecutive days for which FWI is above the local historical (1979–2014) 90th percentile (FWIxCD90).

Extremes in fire weather intensity and duration are analysed independently at all target grid points. To avoid constraining the spatial definition of extreme fire weather at each target grid point, and to account for model noise, spatial maxima are determined in FWIx7day and FWIxCD90 within a predefined area. Ideally, spatial maxima should be taken across a climatologically homogeneous region (Philip et al., 2020), but for a global analysis, the definition needs to remain consistent. In an assessment of observed trends in fire weather extremes (also performed independently at each grid point), Liu et al. (2022a, 2022b) considered annual maxima within a surrounding spatial domain defined by a longitude-latitude box. Arguably, such a definition is unsuitable when applied at the global scale given that the actual size of the spatial domain defined by longitude differs substantially between the equator and the poles. Here, for each target grid point, we determine the maxima in FWIx7day and FWIxCD90 across all grid points within 250 km. Note that our results do not significantly change using a 3-, 5- and 10-day running average to estimate fire weather intensity (not shown). Similarly, for the extreme fire weather duration, our results do not significantly change using the 95th percentile to calculate the number of consecutive days above an extreme threshold (not shown).

## 2.2. Data

Simulations of the historical FWI data are derived from CMIP6 models, which differ considerably in terms of ensemble size. To ensure that the most extreme events are sufficiently well captured, we selected a subset of models with an ensemble size of at least 10 members for the period 1850–2014. The definition for a large ensemble is unclear; in the case of CMIP6, the number of available realizations ranges between 1 and 50. Here, a threshold of 10 realizations is taken, which results in a subset of six ensembles, details are given in Table 1. While the ensemble size varies within our subset (from 10 for CNRM-ESM2-1, INM-CM-5-0 and MPI-ESM1-2-HR to 50 for CanESM5), we do not anticipate strong differences in the representation of internal variability. A threshold of 10 realizations also offers comparative consistency with the ensemble size of other models used in probabilistic attribution of fire weather extremes (e.g., Krikken et al., 2021). Model performance can have considerable spatio-temporal dependency, and these six models have previously been shown to exhibit comparative strengths and weaknesses with respect to the representation of fire weather at regional scales (Gallo et al., 2023). In this sense, the six large ensembles offer a reasonable approximation of the full range of performance across CMIP6.

FWI was calculated for each ensemble using the R package *cffdrs* (Wang et al., 2017). FWI is typically defined by observations of temperature, relative humidity and wind speed recording at noon local time, in addition to 24-h cumulative precipitation. To ensure a consistency across the global analysis, daily values of maximum temperature, minimum relative humidity, mean surface wind speed and total precipitation are taken as proxies for noon conditions. Such an approximation has previously been applied in the derivation of CFWIS indicators from climate models (e.g., Jolly et al., 2015; Calheiros et al., 2022; Gallo et al., 2023).

Data from the Global ECMWF Fire Forecast model (hereafter GEFF-

**Table 1**  
Details of the six CMIP6 models used in the analysis.

Model	Institution	Members	Resolution	Reference
Canadian Earth System Model version 5 (CanESM5)	Canadian Centre for Climate Modelling and Analysis (CCCma)	50	128 × 64 ~ 2.8°	Swart et al. (2019)
Atmosphere-Ocean General Circulation Model (CNRM-CM6-1)	Centre National de Recherches Météorologiques (CNRM)	30	256 × 128 ~ 1.4°	Voldoire et al. (2019)
the Earth system (ES) model of the second generation (CNRM-ESM2-1)	Centre National de Recherches Météorologiques (CNRM)	10	256 × 128 ~ 1.4°	Séférian et al. (2019)
the fifth generation of the INMCM climate model (INM-CM-5-0)	Institute for Numerical Mathematics (INM) of the Russian Academy of Sciences	10	180 × 120 2 × 1.5°	Volodin and Gritsun (2018)
the latest version of the IPSL climate model (IPSL-CM6A-LR)	Institut Pierre-Simon Laplace Climate Modelling Centre (IPSL CMC)	32	144 × 143 ~ 2.5 × 1.3°	Boucher et al. (2020)
the Earth System Model version 1.2 (MPI-ESM1-2-HR)	Max Planck Institute for Meteorology (MPI-M)	10	384 × 192 ~ 0.9°	Müller et al. (2018)

ERA5) (Vitolo et al., 2020) is used as an observational reference for the period 1979–2020. GEF-ERA5 is produced by the European Forest Fire Information System of the Copernicus Emergency Management Service and provides daily FWI data driven by input fields from the ERA5 Reanalysis (ERA5; Hersbach et al., 2020). GEF-ERA5 has been shown to be a realistic representation of real-world day-to-day conditions in previous work (e.g., McElhinny et al., 2020; Gallo et al., 2023) and is an appropriate reference against which model outputs are compared (see Section 2.4 in detail). We note the discrepancy between how FWI is determined in GEF-ERA5 and derivation of FWI in the CMIP6 ensembles, in which the four meteorological components are taken as proxies for noon conditions. However, a comparison of FWI from GEF-ERA5 and FWI calculated independently using the four meteorological components from ERA5 (mirroring the approach applied to CMIP6) found little difference between the two (Gallo et al., 2023). It should also be noted that, by default, GEF-ERA5 does not implement overwintering and that the user is free to determine the start and duration of the fire season (Vitolo et al., 2020; Liu et al., 2022a, 2022b). Our derivation of FWI from the CMIP6 ensembles is consistent with this setup.

To limit the attribution analysis to ‘fire-prone’ regions only, we use an observational dataset to isolate only those areas where evidence of past fires has been recorded. Monthly burned area data from the Global Fire Emissions Database Version 4 (GFED4; Randerson et al., 2018) were used to identify fire-prone grid points. A 9-point smoothing with a quadrilateral curvilinear grid of GFED4 data on each grid point was employed to account for the spatial randomness of fire occurrence during the relatively short period for which GFED4 data is available (1996–2016; van der Werf et al., 2017).

### 2.3. Methodology

A probabilistic framework based on extreme value theory is used to estimate changes in the probability of extreme fire weather. Annual maxima of both intensity (FWIx7day) and duration (FWIxCD90) across all 165 years and all ensemble members from models are pooled and fitted to the GEV distribution. To investigate the dependence of the fit on global warming, both the FWIx7day and FWIxCD90 distributions are scaled with the corresponding 48-month running average in the historical externally forced global mean surface temperature anomalies (GMSTA), which is defined as the ensemble mean of each CMIP6 model as proposed in Deser et al. (2014). In contrast to taking GMSTA for each ensemble member, this approach facilitates the estimation of responsiveness to externally forced global temperature changes. The scaled (and thus non-stationary) distribution is constructed under the assumption that the location parameter  $\mu$  and the scale parameter  $\sigma$  have the same exponential dependency on externally forced GMSTA, for which the ‘dispersion’ ratio  $\sigma/\mu$  and the shape parameter  $\xi$  remain constant (e.g., van der Wiel et al., 2017; van Oldenborgh et al., 2018; Otto et al., 2018; Eden et al., 2018; Krikken et al., 2021; Philip et al., 2020):

$$\mu = \mu_0 \cdot \exp\left(\frac{\alpha T}{\mu_0}\right) \quad (1)$$

$$\sigma = \sigma_0 \cdot \exp\left(\frac{\alpha T}{\mu_0}\right) \quad (2)$$

where  $\mu_0$  and  $\sigma_0$  are the fit parameters of the stationary GEV distribution;  $\alpha$ , as a function of four-year smoothed GMST anomaly  $T$ , represents the trend in fire indicator maxima. The three parameters  $\mu$ ,  $\sigma$  and  $\xi$  indicate the mean, the variability in the tail and the bound of the tail of the distribution, separately. In this case, the exponential dependence on the covariate serves as a convenient method to ensure a distribution that starts from zero and avoids negative FWI values (van Oldenborgh et al., 2021a). At each grid point, probabilities  $p0$  and  $p1$  of a given fire weather extreme occurring in periods of low and high externally forced changes in GMSTA, *i.e.*, low and high anthropogenic forcing

(1880–1884 and 2010–2014 respectively) are estimated. We note that the difference in GMSTA between these two periods differs among the six model ensembles (a range of 0.7 °C to 1.3 °C), to which the results may show some sensitivity. Changes in likelihood, expressed as the ‘probability ratio’ (PR)  $p1/p0$ , are quantified across all fire-prone regions around the world, as identified in the GFED4 dataset. Additionally, changes in extremes in fire weather intensity are expressed as a percentage change in magnitude (%MAG). Correspondingly, changes in extremes in fire weather duration are expressed as a change in the number of consecutive days (durDays).

The scaled GEV approach is well-established and has been previously applied in the context of probabilistic attribution to extremes in heat (e.g., van Oldenborgh et al., 2018; Otto et al., 2018; Eden et al., 2018), precipitation (e.g., van der Wiel et al., 2017) and, more recently to extremes in fire weather intensity (Krikken et al., 2021). Here, for the first time, the approach is also applied to the duration and intensity of extreme fire weather on a global scale. The implementation of the approach also marks its first global application to fire weather extremes from multiple large ensembles of the six CMIP6 models. To ensure that the GEV is a good approximation for FWIx7day and FWIxCD90 data, we performed a goodness of fit test for each (see Figs. S1–S4 in supplementary material). Overall, we found that the GEV exhibits a strong fit when applied to output from model-simulated FWIx7day and FWIxCD90 across more than 99 % and 90 % of the world’s fire-prone areas respectively.

### 2.4. Model evaluation, selection and multi-model synthesis

In order to present the most robust possible assessment of historical changes in extreme fire weather, we present a synthesis of results across the set of model ensembles following a rigorous point-scale evaluation of each model. The ability of climate models to represent a particular type of extreme event is critical and can influence the accuracy and uncertainty of probabilistic attribution analysis (Philip et al., 2020). Here, we evaluate the capacity of each of the six CMIP6 models to represent realistic distributions of fire weather extremes. In line with the approach used in previous work (e.g., van der Wiel et al., 2017; van Oldenborgh et al., 2018; Otto et al., 2018; Eden et al., 2018; Krikken et al., 2021), the basis of this evaluation is the comparison of a stationary GEV distribution (*i.e.*, not scaled by GMSTA) fitted with model-simulated annual maxima and a GEV distribution fitted with corresponding data from the fire danger reanalysis, GEF-ERA5 (Vitolo et al., 2020). Assessment of the similarity of the distribution parameters, and particularly the dispersion ratio and shape parameter of each fit, reflects the suitability of each model at each target grid point. Our pointwise definition of model performance is based on the best estimates of the dispersion ratio and shape parameters of the model stationary GEV fit; sufficiently strong model performance is assumed where those estimates fall within the 95 % confidence intervals of the dispersion ratio and shape parameter from the ‘observed’ GEV fit (fitted with GEF-ERA5 data) following a 1000-sample non-parametric bootstrapping method (Efron and Tibshirani, 1998; van der Wiel et al., 2017).

Combining results from different models for probabilistic attribution often relies on a conventional averaging of results across multiple models, without explicit consideration of the extent of inter-model spread or individual model performance. Here, we present a selective synthesis of model results in which, for each grid point, results are combined across those models that meet the evaluation criteria.

## 3. Results

Focus is initially given to model evaluation and detection of changes in the probability of extreme fire weather intensity (Section 3.1) and duration (Section 3.2). This is followed by point-wise model selection and a multi-model synthesis, identifying regions where changes in the probability of extreme fire weather intensity and duration are the more/

least robust across the different climate model large ensembles model agreement (Section 3.3). All the results are made throughout the world's fire-prone regions.

### 3.1. Extremes in fire weather intensity

#### 3.1.1. Model performance in simulating the extremes in fire weather intensity

To obtain a preliminary insight into the performance of the six CMIP6 large ensembles, simulated global patterns of both the dispersion ratio ( $\sigma/\mu$ ) and shape parameter ( $\xi$ ) for GEV distribution fitted with

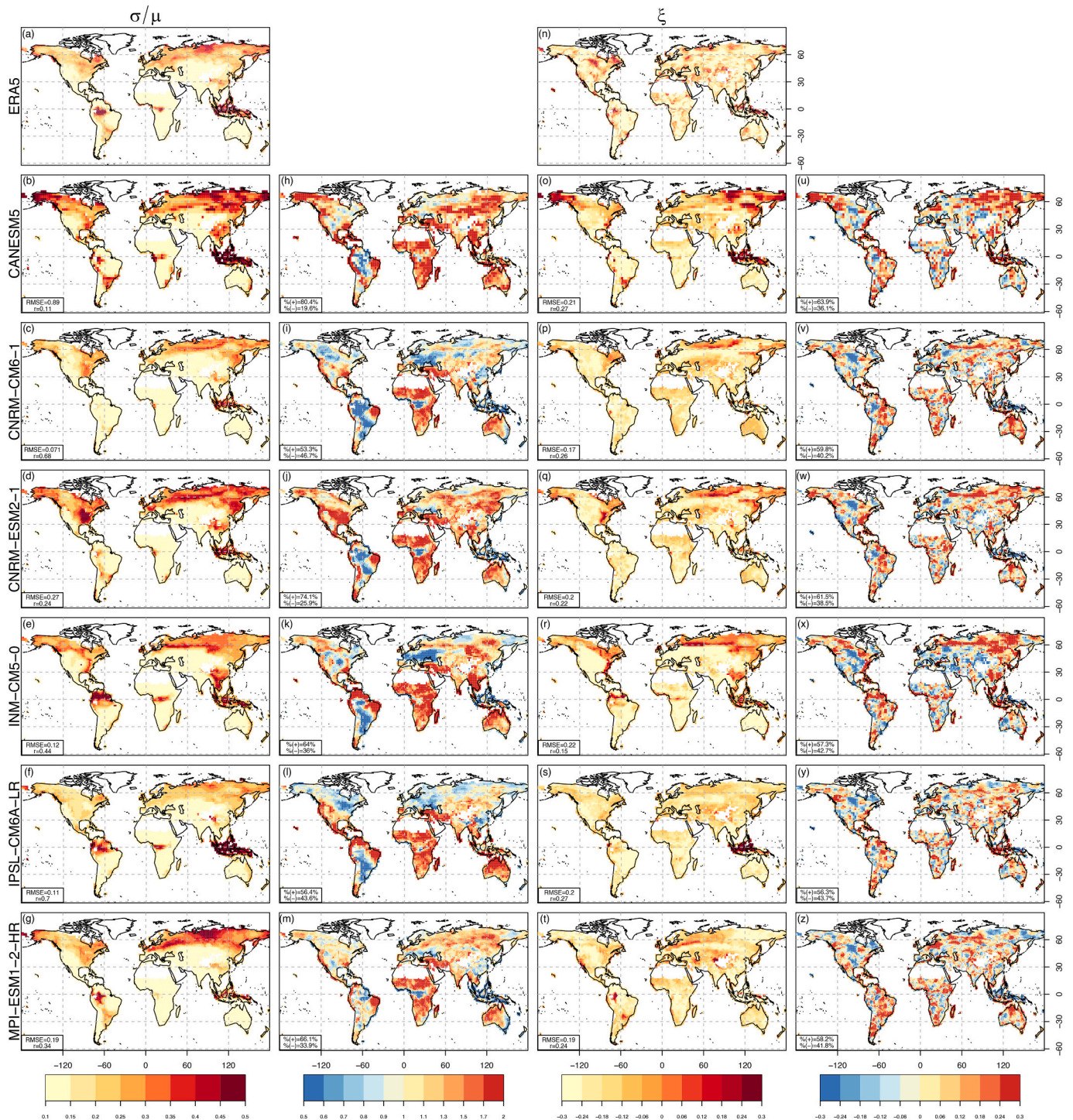


**Fig. 1.** Dispersion ratio ( $\sigma/\mu$ ) derived from the stationary GEV fitted with FWI<sub>x7day</sub> for the period 1979 to 2014 from the GEF5-ERA5 reanalysis (a) and six CMIP6 ensembles (b-g); corresponding differences between the reanalysis and the six CMIP6 models are shown from (h) to (m). Similarly, Shape parameter ( $\xi$ ) from the GEF5-ERA5 reanalysis (n) and six CMIP6 ensembles (o-t) with corresponding differences between the reanalysis and the six CMIP6 models from (u-z). Values in the bottom-left corner of each panel from (b-g) and (o-t) show the root mean square error (RMSE) and spatial correlation coefficient (r) of each six CMIP6 ensembles; while that from (h-m) and (u-z) show the percentage of overestimations (%+) and underestimations (%-) among all the grid cells.

FWIx7day, are compared with the GEF-ERA5 reanalysis for the period from 1979 to 2014, with corresponding differences all shown in Fig. 1.

Concerning the dispersion ratio, GEF-ERA5 produces high values in northwestern and northeastern North America, some parts of equatorial South America, equatorial Africa, and northern and southern Asia (Fig. 1a). According to the root-mean-square errors (RMSE) and spatial correlation ( $r$ ) between the reanalysis and models, CNRM-CM6-1 (Fig. 1c) and IPSL-CM6A-LR (Fig. 1f) show reasonable level of agreements ( $r \sim 0.7$ ) with GEF-ERA5 in many fire-prone regions of the world, despite the apparent inter-model differences in northern South America, equatorial Africa and northern Asia, while CanESM5 produces the lowest correlation (Fig. 1b). CNRM-ESM2-1 (Fig. 1d), INM-CM5-0 (Fig. 1e) and MPI-ESM1-2-HR (Fig. 1g) display a certain degree of similarity with GEF-ERA5 ( $0.2 < r < 0.5$ ), although they still overestimate (%+) > 50 % the dispersion ratio, particularly around equatorial and southern South Africa, Central Asia (Fig. 1j, k & m). The highest overestimates (>80 %; CanESM5) of the extent of the dispersion ratio are shown in northern and southern North America, central and southern Asia, northwest, and southeast Australia (Fig. 1h). It is worth noting that there are apparent underestimations across eastern Europe presented by CNRM-CM6-1 (Fig. 1c), INM-CM5-0 and IPSL-CM6A-LR (Fig. 1i, l & k).

Concerning the shape parameter ( $\xi$ ) of the GEV fitted with GEF-ERA5 maxima, the highest values appear in central and eastern North America, northern Europe, and some parts of northern and southern Asia (Fig. 1n). CanESM5, CNRM-CM6-1 and IPSL-CM6A-LR are the most consistent models when compared with the GEF-ERA5 data, exhibiting relatively small RMSE and a strong spatial correlation ( $r$ ) when compared with the other ensembles (Fig. 1o, p & s), while INM-CM5-0 produced the largest RMSE values (0.22) and the weakest spatial correlation (0.15; Fig. 1r). The other two models, CNRM-ESM2-1 and MPI-ESM1-2-HR, show similar results in terms of RMSE and spatial correlation, with inter-model differences especially apparent in northwestern and eastern North America, central Europe and northeastern Asia (Fig. 1q & t). Fig. 1u-z shows the spatial differences between GEF-ERA5 and the models with the shape parameter overestimated in most of the world, indicating a heavier tail behavior related to the extremes in the distribution. Again, CanESM5 (Fig. 1u) and CNRM-ESM2-1 (Fig. 1w) show the highest degree of overestimations (>60 %), mainly in northern Asia. In general, the representation of the shape parameter in the models is generally less spatially consistent than that of the dispersion ratio.

In summary, the distribution of annual maxima taken from the CMIP6 ensembles is in reasonable agreement with that of GEF-ERA5 annual maxima, although there are some notable differences at the regional scale. Compared to GEF-ERA5, CNRM-CM6-1 and IPSL-CM6A-LR are the best-performing of the six climate models in terms of their representation of the dispersion ratio and shape parameter. CanESM5 and INM-CM5-0 show the lowest-performing skills among the six CMIP6 models, as already shown using different FWI statistics in Gallo et al. (2023).

### 3.1.2. Historical changes in extreme fire weather intensity

Based on the global probabilistic method introduced in Section 2.3, the changes in the likelihood of extreme fire weather (FWIx7day) related to externally forced historical changes in GMSTA are quantified using the GEV-scaling method for each climate model. For each grid box, the 95th percentile of the annual maxima in modelled extreme fire weather from 1850 to 2014 was chosen as a threshold defining extremes, from which we estimated the return level of events. Global maps showing the probability ratio (PR) and change in magnitude (%MAG) between periods of low and high historical anthropogenic forcing are presented in Fig. 2.

Overall, there are several similarities in spatial patterns of both PR and %MAG across the six CMIP6 large ensembles. In relation to externally forced global warming, a 2-fold increase in the probability (PR > 2) of extreme fire weather is found in many regions across the globe,

such as central and southern North America, northern South America, and southern Africa (Fig. 2a-f). This corresponds to an increase of at least 10 % in the magnitude of extreme fire weather (Fig. 2g-l). Regions with increasing likelihoods in %MAG are mainly like those identified in PR for each model. In contrast, regarding the probability of extreme fire weather conditions, northern North America, central Africa and Southeast Asia reflect a decrease in likelihood (PR < 1) across all six climate models (Fig. 2a-f). Note that these simulated decreases in the probability of extreme fire weather conditions, which are here found to be related to historical externally forced warming in GMSTA, are generally in line with the results of observed global fire weather associated with climate change (Liu et al., 2022a). The decreases are likely due to the fact that the regional impacts of climate change are influenced not only by the global warming temperatures but also by other climatic variables, such as precipitation patterns and atmospheric moisture content, which are particularly significant in high-latitude areas of the Northern Hemisphere and in warm and humid tropical regions (Liu et al., 2022a).

There are some similarities in the spatial patterns across the six CMIP6 models, but many areas show sensitivity to the choice of model. For instance, CanESM5, INM-CM5-0 and, particularly, IPSL-CM6A-LR show a strong decrease in the likelihood (PR < 1) of FWIx7day over northern North America (Fig. 2a, d & e), while other models present a relatively small increase in the likelihood of such conditions (PR > 1; Fig. 2b, c & f). The CNRM-CM6-1 and INM-CM5-0 models are the only ones showing a decrease in the likelihood of extreme fire weather in central North America (Fig. 2b) and in many parts of South America (Fig. 2d), respectively. Such discrepancies between models are also found in northern and central Asia: i) decreasing PR over northern Asia and central Asia using CanESM5 (Fig. 2a); ii) decreasing (increasing) PR over northern Asia (Central Asia) using CNRM-ESM2-1 and INM-CM5-0 (Fig. 2c-d); iii) increasing (decreasing) PR are found over northern Asia (Central Asia) in CNRM-CM6-1 (Fig. 2b); iv) IPSL-CM6A-LR (MPI-ESM1-2-HR) shows a decreasing (increasing) PR in almost the entirety of northern and central Asia (Fig. 2e-f). In Australia, such discrepancies also exist: an increase in likelihood can be found in most areas in CanESM5, CNRM-ESM2-1 and IPSL-CM6A-LR (Fig. 2a, c & e), while other models show a combination of increased and decreased change in likelihood (Fig. 2b, d & f). It should be noted that, especially for small changes, the uncertainty range on PR and %MAG, which is not explicitly estimated here, may cross the threshold of positive and negative tendency. This also applies to the PR and durDays results presented in the following section.

The best-performing models for extreme fire weather intensity, CNRM-CM6-1 and IPSL-CM6A-LR, demonstrate similar PR results, with an increase in likelihood of approximately 1.3 and 1.2 times on a global scale, respectively. While southern North America, South America, Africa, equatorial Asia and Australia exhibit similar PR results, notable disparities are observed in northern North America and most of Asia, highlighting the sensitivity of the PR results to the choice of climate models.

### 3.2. Extremes in fire weather duration

#### 3.2.1. Model performance in simulating the extremes in fire weather duration

To assess the performance of the six CMIP6 large ensembles in representing the distribution of extremes in fire weather duration, simulated global patterns for individual parameters of a stationary GEV distribution fitted with FWIxCD90 were compared to distribution parameters from GEF-ERA5 over the period 1979–2014 (Fig. 3).

Regarding their capacity to realistically simulate the distribution of FWIxCD90, CMIP6 models produce GEV parameters that compare reasonably well with the GEF-ERA5 reanalysis. Looking at the dispersion ratio, correlation results show values between 0.3 and 0.7 across most of the world (Fig. 3a-g). All models except for IPSL-CM6A-LR reproduce spatial variability relatively well ( $r > 0.5$ ), with regional

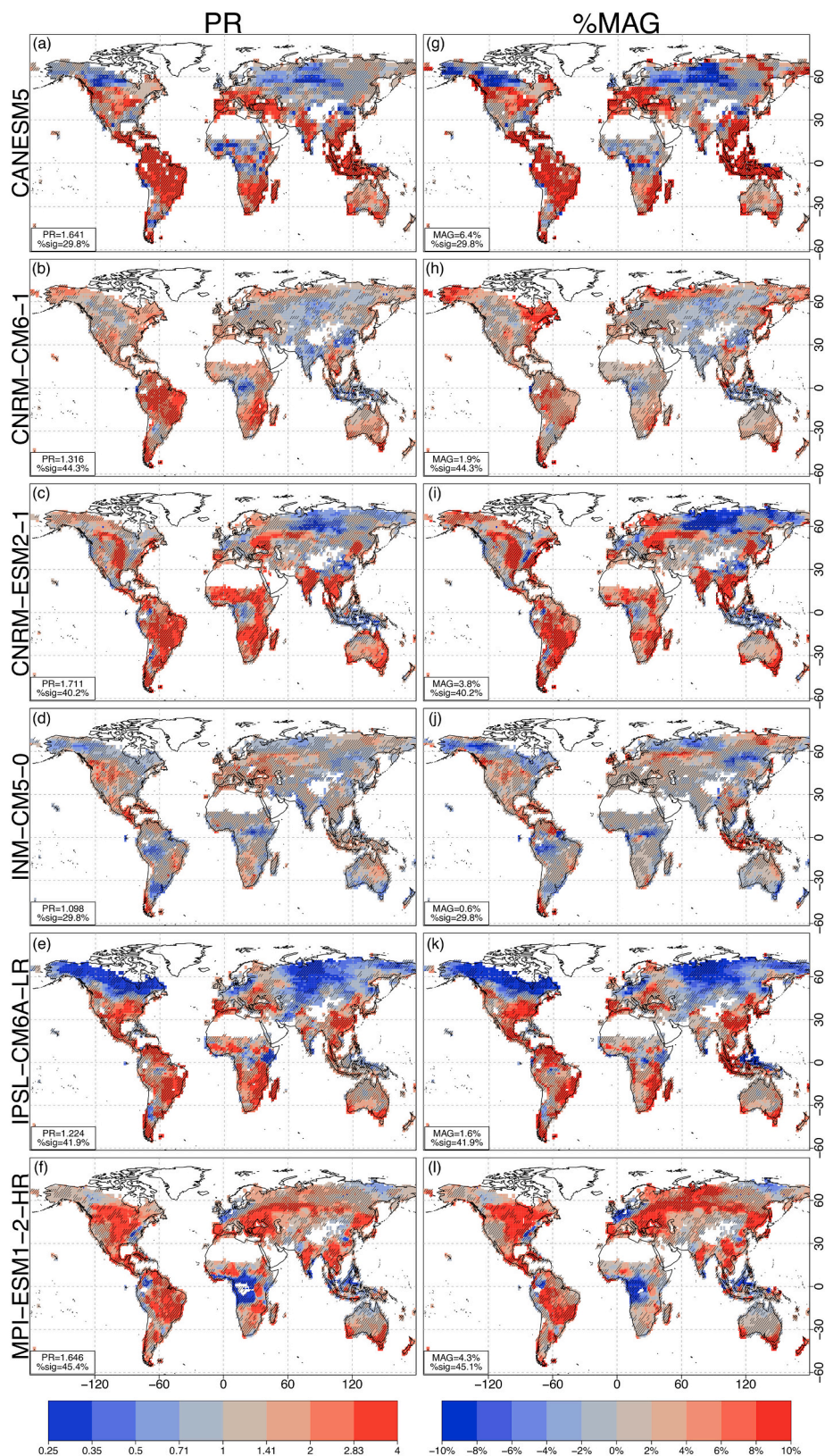


**Fig. 2.** Global maps showing probability ratio (PR; left) and percentage change (%MAG; right) in extremes in FWix7day for six CMIP6 models. The non-stippled areas indicate where the best estimates for the dispersion ratio and shape parameter of the stationary GEV fitted with model-simulated FWix7day fall within the 95 % confidence interval range for the dispersion ratio of the GEV fitted with GEF-ERA5 data. Numbers in the bottom-left corner represent the globally averaged PR (left) and %MAG (right), and the percentage of the burnable world (%sig) for which PR and %MAG results passed the evaluation.

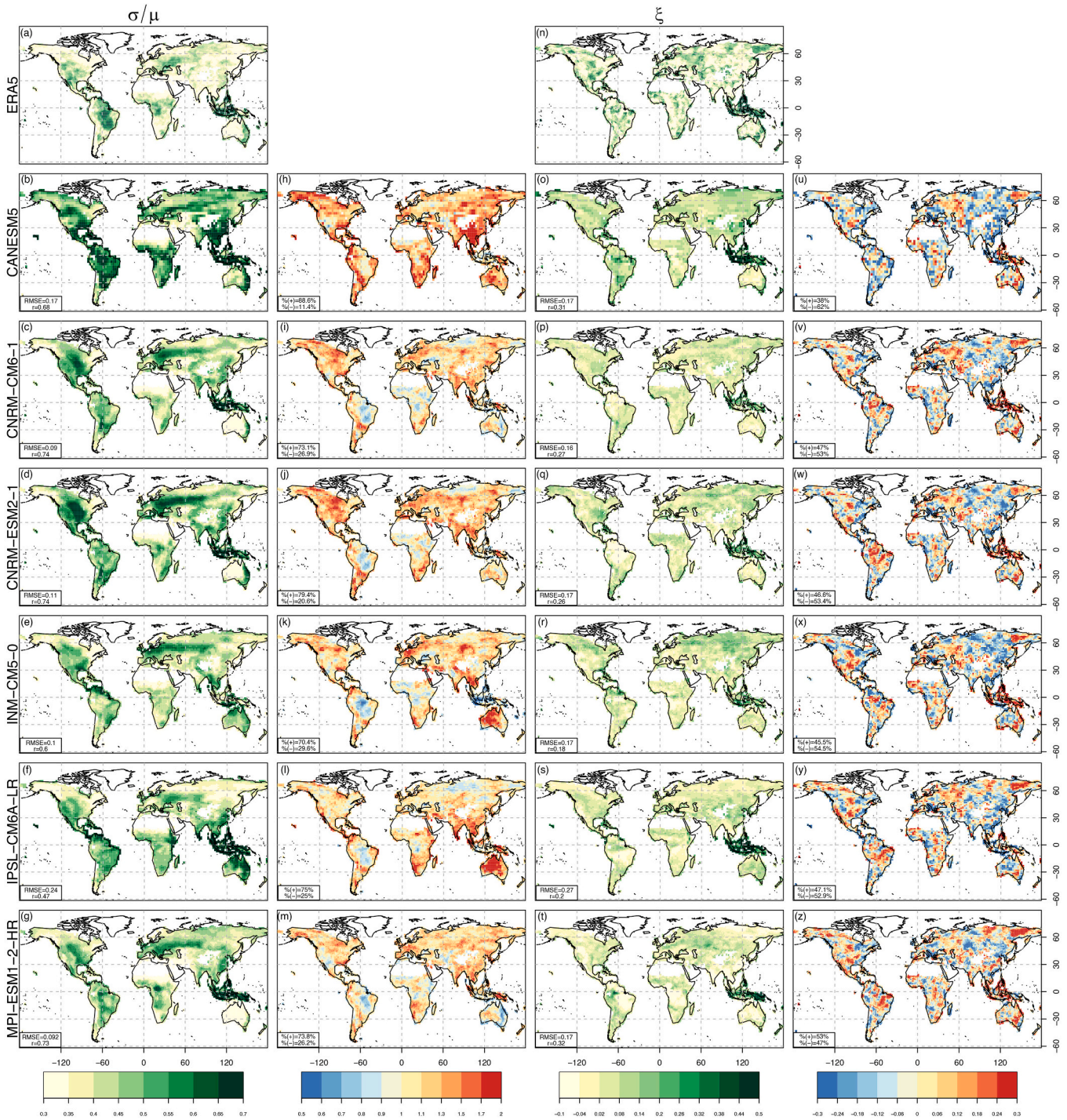


**Fig. 3.** Dispersion ratio ( $\sigma/\mu$ ) and shape parameter ( $\xi$ ) derived from the stationary GEV fitted with FWI<sub>x</sub>CD90 for the period 1979 to 2014 from the GEF-ERA5 reanalysis (a) and six CMIP6 ensembles (b-g); corresponding differences between the reanalysis and the six CMIP6 models are shown from (h) to (m). Similarly, Shape parameter ( $\xi$ ) from the GEF-ERA5 reanalysis (n) and six CMIP6 ensembles (o-t) with corresponding differences between the reanalysis and the six CMIP6 models from (u-z). Values in the bottom-left corner of each panel from (b-g) and (o-t) show the root mean square error (RMSE) and spatial correlation coefficient ( $r$ ) of each six CMIP6 ensembles; while that from (h-m) and (u-z) show the percentage of overestimations (%+) and underestimations (%) among all the grid cells.

differences most apparent in northern North America and South America, northern and southern Asia (Fig. 3a-g). Regions associated with high values of dispersion ratio (as identified in GEF-ERA5), including central and southern North America, eastern Europe, northwestern Asia, and equatorial Asia, are reproduced well by CNRM-CM6-1 (Fig. 3c), CNRM-ESM2-1 (Fig. 3d), INM-CM5-0 (Fig. 3e) and MPI-ESM1-2-HR (Fig. 3g). CanESM5 overestimates the dispersion ratio in almost all the fire-prone

regions (>80 %; Fig. 3h), with the exception of central South America. Meanwhile, the other five models underestimate the dispersion ratio (Fig. 3i-m). Substantial overestimations of the dispersion ratio are also found over most of Australia in INM-CM5-0 (Fig. 3k) and IPSL-CM6A-LR (Fig. 3l), while underestimations are found in CNRM-CM6-1 (Fig. 3i), CNRM-ESM2-1 (Fig. 3j), and MPI-ESM1-2-HR (Fig. 3m) over eastern Australia.

For the shape parameter, GEF-ERA5 displays a substantial variation worldwide (Fig. 3n). Corresponding spatial correlations between the observations and the six models show some level of agreement, with the highest correlation (greater than 0.3) reproduced by CanESM5 (Fig. 3o) and MPI-ESM1-2-HR (Fig. 3t). Five of the six models show underestimations that are greater than 50 % over all grid cells, mainly scattered around southern South Africa, North and Central Asia (Fig. 3u-z). The only exception is MPI-ESM1-2-HR (Fig. 3z), with strong overestimation in eastern South Africa and northeast Asia.

Concerning the dispersion ratio and shape parameter in the distribution, CNRM-CM6-1, CNRM-ESM2-1 and MPI-ESM1-2 are the best-performing of the six climate models, when compared to GEF-ERA5. IPSL-CM6A-LR is the most biased among the six models. The findings align closely with those of the study by Gallo et al. (2023), with MPI-ESM1-2-HR demonstrating one of the highest model skills in simulating fire weather conditions. Also, as in Gallo et al. (2023), CNRM-CM6-1 and CNRM-ESM2-1 exhibit relatively strong performances, while IPSL-CM6-LR shows relatively poor performance compared to a theoretical average model.

### 3.2.2. Historical changes in extreme fire weather duration

Fig. 4(a)-(l) shows a global map of the probability ratio (PR) and change in FWixCD90 (durDays) at each grid point across the six CMIP6 models. Overall, for the period 2010–2014, the probability of more prolonged extreme fire weather conditions has markedly risen by a factor of two on a global scale compared to the 1880–1884 period (Fig. 4a-f). This equates to an increase of at least 10 days in the maximum duration of extreme fire weather events in relation to externally forced temperature rise (Fig. 4g-l). In particular, the most pronounced increases in the likelihood of more prolonged extreme fire weather occur in southern North America, almost all South America, southern Africa, Central and Southeast Asia and parts of Australia (Fig. 4a-f). However, we note that northern North America (CanESM5 and IPSL-CM6A-LR; Fig. 4a & e) and equatorial Africa (CNRM-CM6-1, CNRM-ESM2-1 and MPI-ESM1-2-HR; Fig. 4b, c, f) are associated with a substantial (up to fourfold) decrease in the likelihood of FWixCD90. This indicates that in these models the maximum duration of extreme fire weather tends to decrease in relation to historical externally forced warming in GMSTA, aligning with the changes in the intensity of fire weather extremes (Section 3.1.2). This can be attributed to various impacts of climate change, including changes in precipitation and relative humidity, but this does not suggest that extreme fire weather events are unrelated to human-driven climate change (Liu et al., 2022a).

We also note regional divergence in the simulated changes in the maximum duration of extreme fire weather that is associated with historical changes in externally forced GMSTA. For central North America, western and southern Europe, the maximum duration of extreme fire weather simulated by CanESM5, INM-CM5-0, IPSL-CM6A-LR and MPI-ESM1-2-HR shows an upward trend in PR (Fig. 4a, d, e & f), while a downward trend in PR is found using CNRM-CM6-1 and CNRM-ESM2-1 (Fig. 4b & c). This regional divergence between climate models is more common in Asia. For example, in northern Asia, where wildfires occur more prevalently, CNRM-CM6-1, IPSL-CM6A-LR and MPI-ESM1-2-HR show a significant increase in the likelihood of maximum duration of extreme fire weather (Fig. 4b, e & f), but the other three models show the opposite change in likelihood (Fig. 4a, c & d). These patterns and deviations in regional distribution also appear in Australia, with most regions showing a potential increase in the likelihood of more prolonged extreme fire weather conditions (Fig. 4a, b, c & e). Meanwhile, some models, such as INM-CM5-0 or MPI-ESM1-2-HR (Fig. 4d, f), suggest a decreasing probability of prolonged extreme fire weather conditions in the southern or northern regions of Australia.

Similarly, the best performing models for extreme fire weather duration, CNRM-CM6-1, CNRM-ESM2-1, and MPI-ESM1-2-HR, exhibit relatively consistent PR results, with the increase in likelihood of approximately 1.3, 1.4, and 1.5 times on a global scale, respectively.

While South America, Africa, Equatorial Asia, and Australia demonstrate similar patterns of PR increase and decrease, notable variations are evident across numerous regions worldwide, notably in southern North America and Southeast Asia.

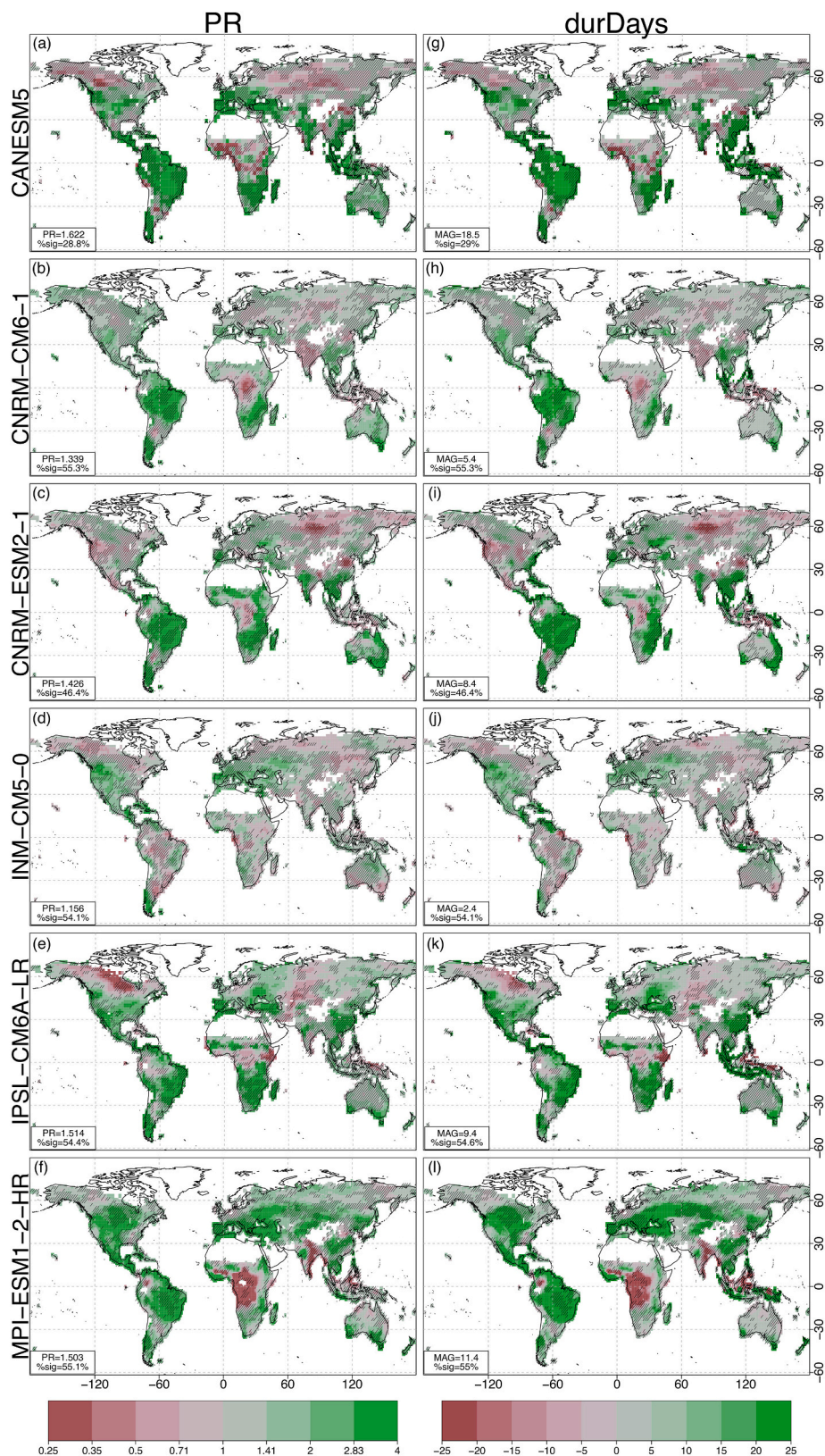
### 3.3. Attribution synthesis across multiple models

In this subsection, we firstly assess consensus among the six CMIP6 large ensembles, and secondly, explore the value of a model evaluation and selection step in synthesising multi-model attribution results. Fig. 5 summarises to what extent the six CMIP6 models agree on the tendency of the change in likelihood in extremes of fire weather intensity (Fig. 5a) and duration (Fig. 5b). The result suggests that, in relation to the externally forced warming GMSTA, 54.3 % of the grid cells show an increased likelihood of both extreme fire weather intensity and duration when the number of model agreements is larger than three. All models simulate an increased likelihood of prolonged and high-intensity events in large parts of the world's fire-prone regions, including areas that have witnessed severe fire episodes in recent years (most notably southern Europe). An increase in likelihood in at least five of the six models is apparent across much of the Americas, southern Africa, Australia, and eastern Asia. Models agree on an increased likelihood of prolonged extreme fire weather episodes, but there is less consensus on the change in intensity. Regions of the lower model agreement include large parts of the boreal forests and Canada and Eurasia, particularly for intensity, in addition to central Africa and Southeast Asia.

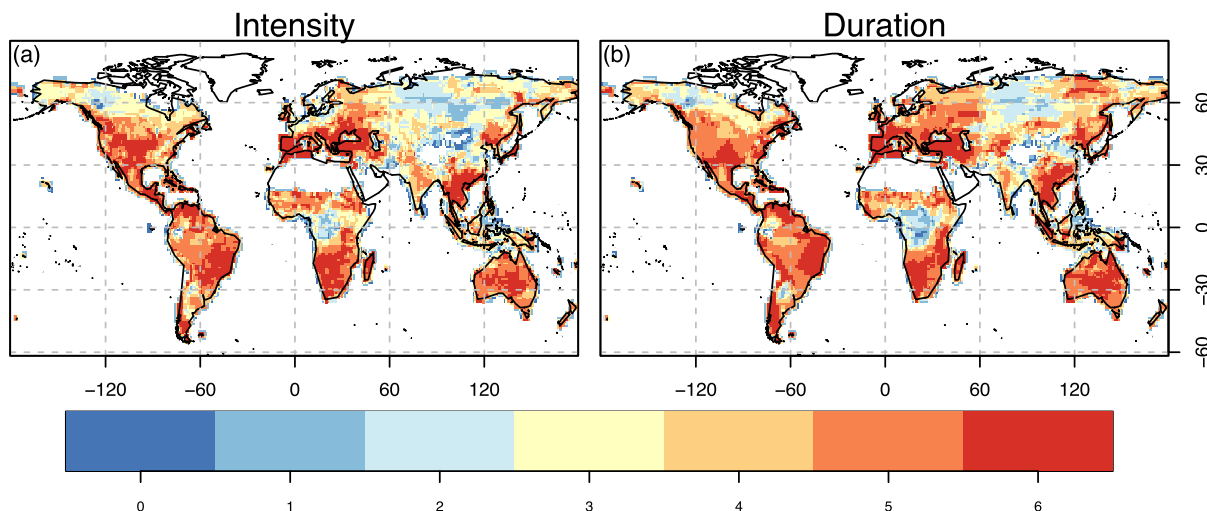
As discussed by Liu et al. (2022a), the use of a common method and event definition allows for the robust detection of changes at various locations and from multiple data sources to be combined. However, combining statistics from different climate models may prove troublesome if there are clear differences in model performance. Fig. 5 demonstrates a regional dependence in model agreement. It is important to understand the extent to which such discrepancies are due to model performance for the climate impact assessment, so to be as robust as possible. Here, we apply a model evaluation and selection to identify models that can realistically reproduce the dispersion and the shape of the distribution of fire weather extremes. All models that meet the evaluation criteria can, therefore, be combined to produce global attribution results that, in principle, are more robust and reliable than those that would be produced by combining the results of all models irrespective of their performance.

Fig. 6 illustrates multi-model global probability ratio maps constructed, firstly, from a conventional averaging of the probability ratios simulated by all six CMIP6 models irrespective of model performance (Fig. 6a-b) and, secondly, using a selective averaging of models that pass the evaluation criterion (Fig. 6c-d). As explained in Section 2.4, the evaluation criterion is defined by the best estimates of the dispersion ratio and shape parameters of the model stationary GEV fit; where those estimates fall within the range of the 95 % confidence intervals for the dispersion ratio and shape parameter of the GEV fitted by GEF-ERA5 data, the model is selected for the multi-model synthesis.

The global PR map (Fig. 6a-b), based on the first, conventional synthesis, shows relatively small changes in the probability of extremes in both FWix7day and FWixCD90. Only a few regions, such as northern South America, southern Africa, and southern Asia, show an approximately two-fold increase in the probability of the fire weather extremes in both intensity and duration of days. There are no particularly strong or prominent trends, especially in the areas with decreasing probabilities, which are only present in a small part of the equatorial region of Africa. However, the conventional synthesis may underestimate the range of probabilities to some extent compared to the selective synthesis, which is shown in Fig. 6c-d. In contrast to the conventional synthesis, the selective approach considers the individual performance of each model and combines the results of those that perform well. The outcomes show an even more remarkable degree of variability, with southern North America, south-eastern Europe and southwestern and



**Fig. 4.** Global maps showing probability ratio (PR; left) and the absolute changes (durDays; right) in FWixCD90 for the six CMIP6 models. The non-stippled areas indicate where the best estimates for the dispersion ratio and shape parameter of the stationary GEV fitted with model-simulated FWixCD90 falls within the 95 % confidence interval range for the dispersion ratio of the GEV fitted with GEF-ERA5 data. Numbers in the bottom-left corner represent the globally averaged PR (left) and durDays (right), and the percentage of the burnable world (%sig) for which PR and %MAG results passed the evaluation.



**Fig. 5.** Maps showing the number of climate models that present an increased likelihood of extremes in (a) fire weather intensity and (b) fire weather duration across the six CMIP6 models. Results are interpolated to a  $384 \times 192$  ( $\sim 0.9^\circ$ ) grid (which is the highest resolution among the models assessed). Areas approaching red (blue) indicate that an increasing number of models show a positive (negative) change. (For interpretation of the references to colour in this figure legend, the reader is referred to the web version of this article.)

south-eastern Australia exhibiting an apparent rise in PR of approximately four times to the fire weather extremes in intensity and duration (Fig. 6c-d), in addition to northern South America, southern Africa, and southern Asia regions (Fig. 6a-b). Correspondingly, two-fold decreases in the likelihood of the fire weather extremes in both intensity and duration of days are not only encountered in the equatorial regions of Africa previously mentioned (Fig. 6a-b) but are also apparent in northern North America and most parts of northern and central Asia. Notably, changes in PR for both FWIx7day and FWIxCD90 tend to be spatially consistent, *i.e.*, the higher the probability of an increase in fire weather intensity, the longer the duration of the fire weather and, conversely, the lower the intensity the shorter the duration.

Fig. 6e-f displays the difference in PR of extreme fire weather intensity and duration between the conventional and selective approaches. Results following the model evaluation and selection illustrate the extent to which PR differs compared to the conventional synthesis. Of particular note is that, following model selection, the PR for FWIx7day is up to 80 % greater in parts of eastern and southern Europe (Fig. 6e), while the PR for FWIxCD90 is up to 60 % lesser in much of western and central Europe (Fig. 6f).

Concerning each grid cell, the percentage of uncertainty changes in the range of PR (0–100 %) is shown in Fig. 6g-h. The range is provided by the lowest and highest PR among evaluated CMIP6 models, while the change of the range is according to the two synthesis approaches applied in Fig. 6a-d. Overall, the global changes for both extreme fire weather intensity (Fig. 6g) and duration (Fig. 6h) are 45.1 % and 39.1 %, as a decrease in the range of PR, separately. There is a positive trend in the number of grid cells reaching the averaged values (45.1 % for fire weather intensity and 39.1 % for fire weather duration) and a negative trend after that. This statistical analysis manifests the variation in PR ranges between the results of all the six CMIP6 large ensembles. Subsequently, results of the model ensembles that passed the evaluation, clearly reveal the sensitivity of the application of large climate model ensembles and the importance of model evaluation and a selection step.

#### 4. Discussion and conclusions

The occurrence and subsequent impact of severe wildfires in recent years has heightened scientific, public and media curiosity about how such events are linked to a changing climate. Probabilistic attribution studies are an important means to assess the impact of climate change on wildfires but require a distinction to be made between the fire itself and

the meteorological conditions that coincided with it. Studies seeking to link the probability of extreme fire weather to climate change are rare in comparison to, for instance, flood- and drought-related studies. However, as the number of wildfires, or fire weather, climate change impact assessments begin to grow, there is a clear need to continue to build an understanding of historical global and regional changes affecting fire weather, their potential link to climate change, as well as the range of uncertainty associated with the use of climate models, notably CMIP6 models.

Here, using six CMIP6 large ensembles and established statistical methodologies routinely applied in the context of probabilistic attribution, we examined how historical externally forced warming in GMSTA has affected extreme fire weather intensity and duration. While there is substantial variability in model performance in most fire-prone regions of the world, there is a general increase in the likelihood of extreme fire weather occurrence in relation to externally forced warming in GMSTA. This trend is broadly consistent with the current understanding of historical changes in global fire weather activity and its relationship to observation changes in global temperature, particularly for the increases in likelihood across central and southern North America, southern South America, southern Africa and Australia, and the decreases in northern North America and South East Asia (Jain et al., 2022; Liu et al., 2022a). However, for some regions, the discrepancies between models are pronounced, such as the regions across most of Asia, two of the six models show similar increasing trends when compared with the observed changes in FWI, while other models exhibit decreasing trends with the observed changes in other CFWIS components (Liu et al., 2022a). This demonstrates the non-negligible and large uncertainties associated with the use of a single model in probabilistic attribution studies and the importance of integrating results from multiple climate models and examining the performance of model skill. It is also worth noting that in, for example, equatorial rainforest regions, higher relative humidity due to warming temperatures may prevent extreme fire weather from occurring. Further analysis of extremes in such regions might consider alternative fire weather indicators given that FWI and other CFWIS components are not strongly correlated with burned area (Liu et al., 2022a).

Using the same six large ensembles, we then analysed probabilistic changes in extremes in fire weather duration. We found an increasing trend in probabilities of prolonged fire weather extremes across most of the globe, which appears consistent with the increasing probability of high-intensity extreme fire weather conditions. This is accompanied by a

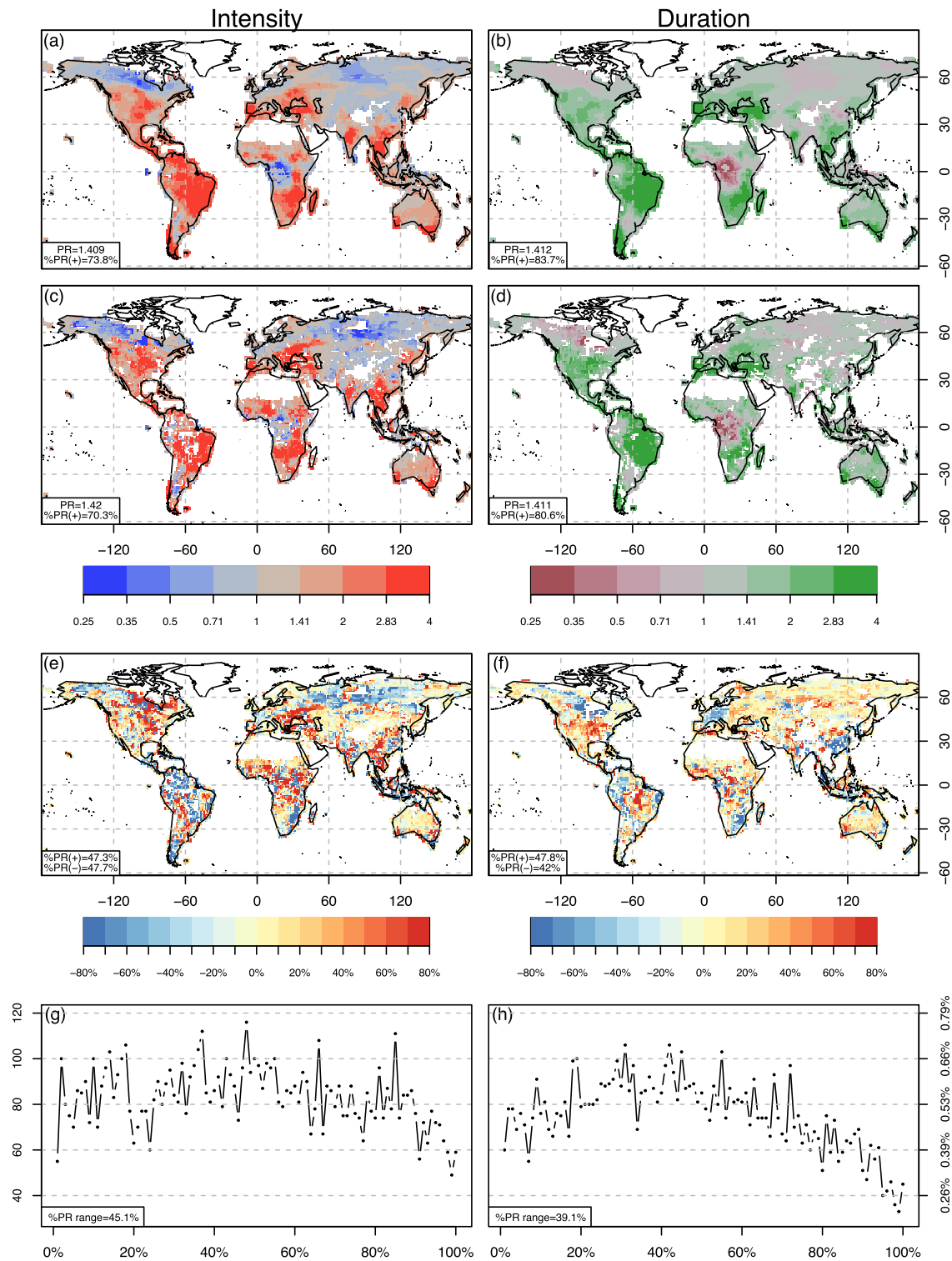


**Fig. 6.** (a-d) Composite plots showing the average PR for trends across (a)-(b) all the six CMIP6 models in FWix7day (a) and FWixCD90 (b); (c)-(d) CMIP6 models that sufficiently well-reproduce the dispersion of the distribution and the parameter of the shape of extremes in FWix7day (c) and FWixCD90 (d). Additional white areas indicate the regions where no climate model met the evaluation criteria. Values in the bottom-left corner of each panel from (a-d) show the globally averaged PR and the percentage of the burnable world that shows an increase in PR (%PR(+)). (e) Changes in the average PR across all the six CMIP6 models (a) and the selected models (c) in FWix7day. (f) as (e) but across all the six CMIP6 models (b) and the selected models (d) in FWixCD90. Numbers in the bottom-left corner represent the percentage of the burnable world that shows an increase (%PR(+)) or decrease (%PR(-)) in PR. (g-h) Line charts for the number of grid cells (left axis) and the percentage (right axis) of uncertainty changes in PR range between the result across all the six CMIP6 models and evaluated results in FWix7day (g) and FWixCD90 (h). Values in the bottom-left corner of each panel show the percentage of the decreasing changes in the PR range across the burnable world.

decreasing trend in probabilities of prolonged fire weather extremes for specific regions, such as northern North America and equatorial Africa. Notably, it was found that the upward trend in the probability of extreme fire weather intensity tends to be paired with an increase in its duration, *i.e.*, the occurrence of more intense fire weather also predicts a greater likelihood of a prolonged duration of the weather phenomenon. We again note substantial differences in model performance through the world's prone regions.

Finally, a synthesis was generated from the results of a selected subset climate models that met performance criteria following a point-by-point evaluation. The results confirm an increasing trend in the probability and duration of extreme fire weather in relation to historical externally forced changes in GMSTA, particularly in southern North America, south-eastern Europe, south-western and south-eastern Australia, where the probability of this increase is up to four times more likely compared with the past fire weather condition. The selective approach to generating a multi-model synthesis produces quite different results to a conventional approach that combines the results of all models irrespective of their performance most notably in fire-prone parts of Europe. Given the additional robustness of the selective approach, these differences clearly support the incorporation of model evaluation and selection in probabilistic attribution analysis.

The results of this study also highlight the sensitivity of the probabilistic attribution, and more widely of climate change impact assessment, in the context of fire weather extremes to the choice of climate models. Single models suffer from unavoidable biases, while a simple combination of multiple models can lead to a significant underestimation of results under some circumstances. As highlighted by previous work focused on trends in observed datasets, quantification of changes in fire weather extremes is sensitive to the choice of fire weather indicator (Liu et al., 2022a, 2022b). FWI is a widely used and understood metric and appropriate for the worldwide analysis presented in this study but is not necessarily the most appropriate indicator when the focus is on a specific location or region. Therefore, the following recommendations are made for future climate change impact assessment in the context of extreme fire weather events: (i) careful consideration and justification of the most appropriate fire weather indicator for the study region; (ii) use of multiple climate model large ensembles; and (iii) robust evaluation of models' capacity to realistically represent the distribution of extreme fire weather statistics.

#### CRedit authorship contribution statement

**Zhongwei Liu:** Writing – review & editing, Writing – original draft, Methodology, Formal analysis. **Jonathan M. Eden:** Writing – review & editing, Supervision. **Bastien Dieppois:** Writing – review & editing, Supervision. **Igor Drobyshev:** Writing – review & editing. **Folmer Krikken:** Writing – review & editing. **Matthew Blackett:** Writing – review & editing, Supervision.

#### Declaration of competing interest

The authors declare that they have no known competing financial interests or personal relationships that could have appeared to influence the work reported in this paper.

#### Data availability

Data will be made available on request.

#### Acknowledgements

The research leading to these results received funding from Centre for Agroecology, Water and Resilience, Coventry University through Trailblazer PhD studentship scheme (Sub Project Code: 13771).

#### Appendix A. Supplementary data

Supplementary data to this article can be found online at <https://doi.org/10.1016/j.gloplacha.2025.104822>.

#### References

- Abatzoglou, J.T., Williams, A.P., Barbero, R., 2019. Global emergence of anthropogenic climate change in fire weather indices. *Geophys. Res. Lett.* 46 (1), 326–336.
- Barnes, C., Boulanger, Y., Keeping, T., Gachon, P., Gillett, N., Boucher, J., Roberge, F., Kew, S., Haas, O., Heinrich, D., Vahlberg, M., Singh, R., Elbe, M., Sivanu, S., Arrighi, J., van Aalst, M., Otto, F., Zacharia, M., Krikken, F., Wang, X., Erni, S., Pietropalo, E., Avis, A., Bisailon, A., Kimutai, J., 2023. Climate Change more than Doubled the Likelihood of Extreme Fire Weather Conditions in Eastern Canada. *World Weather Attribution*, p. 26. <https://doi.org/10.25561/105981>.
- Boer, M.M., Resco de Dios, V., Bradstock, R.A., 2020. Unprecedented burn area of Australian mega forest fires. *Nat. Clim. Change* 10 (3), 171–172.
- Boucher, O., Servonnat, J., Albright, A.L., Aumont, O., Balkanski, Y., Bastrikov, V., Bekki, S., Bonnet, R., Bony, S., Bopp, L., Braconnot, P., 2020. Presentation and evaluation of the IPSL-CM6A-LR climate model. *J. Adv. Model. Earth Syst.* 12 (7), e2019MS002010.
- Bowman, D.M., Kolden, C.A., Abatzoglou, J.T., Johnston, F.H., van der Werf, G.R., Flannigan, M., 2020. Vegetation fires in the Anthropocene. *Nat. Rev. Earth Environ.* 1 (10), 500–515.
- Calheiros, T., Benali, A., Pereira, M., Silva, J., Nunes, J., 2022. Drivers of extreme burnt area in Portugal: fire weather and vegetation. *Nat. Hazards Earth Syst. Sci.* 22, 4019–4037. <https://doi.org/10.5194/nhess-22-4019-2022>.
- Deeming, J.E., 1972. National fire-danger rating system. In: *Rocky Mountain Forest and Range Experiment Station, Forest Service, US Department of Agriculture*, 84.
- Deeming, J.E., Burgan, R.E., Cohen, J.D., 1977. The national fire-danger rating system—1978. In: *Intermountain Forest and Range Experiment Station*, 39. Forest Service, US Department of Agriculture.
- Deser, C., Phillips, A.S., Alexander, M.A., Smoliak, B.V., 2014. Projecting north American climate over the next 50 years: uncertainty due to Internal Variability. *J. Climate* 27 (6), 2271–2296.
- Deser, C., Lehner, F., Rodgers, K.B., Ault, T., Delworth, T.L., DiNezio, P.N., Fiore, A., Frankignoul, C., Fyfe, J.C., Horton, D.E., Kay, J.E., 2020. Insights from Earth system model initial-condition large ensembles and future prospects. *Nat. Clim. Change* 10 (4), 277–286.
- Du, J., Wang, K., Cui, B., 2021. Attribution of the extreme drought-related risk of wildfires in spring 2019 over Southwest China. *Bull. Am. Meteorol. Soc.* 102 (1), S83–S90.
- Eden, J.M., Kew, S.F., Bellprat, O., Lenderink, G., Manola, I., Omrani, H., van Oldenborgh, G.J., 2018. Extreme precipitation in the Netherlands: an event attribution case study. *Weather Clim. Extremes* 21, 90–101.
- Efron, B., Tibshirani, R., 1998. The problem of regions. *Ann. Stat.* 26 (5), 1687–1718.
- Ellis, T.M., Bowman, D.M., Jain, P., Flannigan, M.D., Williamson, G.J., 2022. Global increase in wildfire risk due to climate-driven declines in fuel moisture. *Glob. Chang. Biol.* 28 (4), 1544–1559.
- Gallo, C., Eden, J.M., Dieppois, B., Drobyshev, I., Fulé, P.Z., San-Miguel-Ayanz, J., Blackett, M., 2023. Evaluation of CMIP6 model performances in simulating fire weather spatiotemporal variability on global and regional scales. *Geosci. Model Dev.* 16, 3103–3122.
- Hersbach, H., Bell, B., Berrisford, P., Hirahara, S., Horányi, A., Muñoz-Sabater, J., Nicolas, J., Peubey, C., Radu, R., Schepers, D., Simmons, A., 2020. The ERA5 global reanalysis. *Q. J. Roy. Meteorol. Soc.* 146 (730), 1999–2049.
- Jain, P., Castellanos-Acuna, D., Coogan, S.C., Abatzoglou, J.T., Flannigan, M.D., 2022. Observed increases in extreme fire weather driven by atmospheric humidity and temperature. *Nat. Clim. Change* 12 (1), 63–70.
- Jolly, W., Cochrane, M., Freeborn, P., et al., 2015. Climate-induced variations in global wildfire danger from 1979 to 2013. *Nat Commun* 6, 7537. <https://doi.org/10.1038/ncomms8537>.
- Kimutai, J., Carrasco-Escalf, T., Garreaud, R.D., Zachariah, M., Barnes, C., Libonati, R., Keeping, T., Villarroya Jiménez, C., Muñoz Bravo, F., Boisier, J.P., Santos Vega, M., Vahlberg, M., Sengupta, S., Otto, F., Clarke, B., Muñoz, A., Rojas Corradi, M., Mistry, M., Philip, S., Kew, S., 2024. Despite known coastal cooling trend, risk of deadly wildfires in Central Chile increasing with changing land management in a warming climate. *World Weather Attribution*. 21. <https://doi.org/10.25561/109375>.
- Kirchmeier-Young, M.C., Zwiers, F.W., Gillett, N.P., Cannon, A.J., 2017. Attributing extreme fire risk in Western Canada to human emissions. *Clim. Change* 144 (2), 365–379.
- Kirchmeier-Young, M.C., Gillett, N.P., Zwiers, F.W., Cannon, A.J., Anslow, F.S., 2019. Attribution of the influence of human-induced climate change on an extreme fire season. *Earth's Future* 7 (1), 2–10.
- Krikken, F., Lehner, F., Hausteink, K., Drobyshev, I., van Oldenborgh, G.J., 2021. Attribution of the role of climate change in the forest fires in Sweden 2018. *Natural Hazards Earth Syst. Sci.* 21, 2169–2179.
- Lewis, S.C., Blake, S.A., Trewin, B., Black, M.T., Dowdy, A.J., Perkins-Kirkpatrick, S.E., King, A.D., Sharples, J.J., 2020. Deconstructing factors contributing to the 2018 fire weather in Queensland, Australia. *Bull. Am. Meteorol. Soc.* 101 (1), S115–S122.
- Liu, Z., Eden, J.M., Dieppois, B., Blackett, M., 2022a. A global view of observed changes in fire weather extremes: uncertainties and attribution to climate change. *Clim. Change* 173, 14.

- Liu, Z., Eden, J.M., Dieppois, B., Drobyshev, I., Gallo, C., Blackett, M., 2022b. Were Meteorological Conditions Related to the 2020 Siberia Wildfires made more likely by Anthropogenic climate change? *Bull. Am. Meteorol. Soc.* 103 (3), S44–S49.
- Liu, Z., Eden, J.M., Dieppois, B., Conradie, W.S., Blackett, M., 2023. The April 2021 cape town wildfire: has anthropogenic climate change altered the likelihood of extreme fire weather? *Bull. Am. Meteorol. Soc.* 104 (1), E298–E304.
- Maher, N., Milinski, S., Ludwig, R., 2021. Large ensemble climate model simulations: introduction, overview, and future prospects for utilising multiple types of large ensemble. *Earth Syst. Dynam.* 12, 401–418.
- McArthur, A.G., 1967. Fire behaviour in Eucalypt forests. Leaflet (Australia Forestry Timber Bureau) no. 107.
- McElhinny, M., Beckers, J.F., Hanes, C., Flannigan, M., Jain, P., 2020. A high-resolution reanalysis of global fire weather from 1979 to 2018—overwintering the Drought Code. *Earth Syst. Sci. Data* 12 (3), 1823–1833.
- Milinski, S., Maher, N., Olonscheck, D., 2020. How large does a large ensemble need to be? *Earth Syst. Dynam.* 11, 885–901.
- Müller, W.A., Jungclaus, J.H., Mauritsen, T., Baehr, J., Bittner, M., Budich, R., Bunzel, F., Esch, M., Ghosh, R., Haak, H., Ilyina, T., 2018. A higher-resolution version of the max planck institute earth system model (MPI-ESM1. 2-HR). *J. Adv. Model. Earth Syst.* 10 (7), 1383–1413.
- National Academies of Sciences, Engineering, and Medicine, 2016. Attribution of Extreme Weather Events in the Context of Climate Change. National Academies Press, Washington DC.
- van Oldenborgh, G.J., Philip, S., Kew, S., van Weele, M., Uhe, P., Otto, F., Singh, R., Pai, I., Cullen, H., AchutaRao, K., 2018. Extreme heat in India and anthropogenic climate change. *Nat. Hazards Earth Syst. Sci.* 18, 365–381.
- van Oldenborgh, G.J., Krikken, F., Lewis, S., Leach, N.J., Lehner, F., Saunders, K.R., van Weele, M., Haustein, K., Li, S., Wallom, D., Sparrow, S., 2021a. Attribution of the Australian bushfire risk to anthropogenic climate change. *Natural Hazards Earth Syst. Sci.* 21 (3), 941–960.
- van Oldenborgh, G.J., van der Wiel, K., Kew, S., Philip, S., Otto, F., Vautard, R., King, A., Lott, F., Arrighi, J., Singh, R., van Aalst, M., 2021b. Pathways and pitfalls in extreme event attribution. *Clim. Change* 166 (1), 1–27.
- Otto, F.E., Wolski, P., Lehner, F., Tebaldi, C., Van Oldenborgh, G.J., Hogesteegeer, S., Singh, R., Holden, P., Fućkar, N.S., Odoulami, R.C., New, M., 2018. Anthropogenic influence on the drivers of the Western Cape drought 2015–2017. *Environ. Res. Lett.* 13 (12), 124010.
- Philip, S., Kew, S., van Oldenborgh, G.J., Otto, F., Vautard, R., van der Wiel, K., King, A., Lott, F., Arrighi, J., Singh, R., van Aalst, M., 2020. A protocol for probabilistic extreme event attribution analyses. *Adv. Stat. Climatol. Meteorol. Oceanogr.* 6 (2), 177–203.
- Randerson, J.T., van der Werf, G.R., Giglio, L., Collatz, G.J., Kasibhatla, P.S., 2018. Global Fire Emissions Database, Version 4, (GFEDv4). ORNL DAAC, Oak Ridge, Tennessee, USA. <https://doi.org/10.3334/ORNLLDAAC/1293>.
- Séférian, R., Nabat, P., Michou, M., Saint-Martin, D., Voldoire, A., Colin, J., Decharme, B., Delire, C., Berthet, S., Chevallier, M., Sénési, S., 2019. Evaluation of CNRM earth system model, CNRM-ESM2-1: Role of earth system processes in present-day and future climate. *J. Adv. Model. Earth Syst.* 11 (12), 4182–4227.
- Swart, N.C., Cole, J.N., Kharin, V.V., Lazare, M., Scinocca, J.F., Gillett, N.P., Anstey, J., Arora, V., Christian, J.R., Hanna, S., Jiao, Y., 2019. The Canadian earth system model version 5 (CanESM5. 0.3). *Geosci. Model Dev.* 12 (11), 4823–4873.
- Tett, S.F., Falk, A., Rogers, M., Spuler, F., Turner, C., Wainwright, J., Dimdore-Miles, O., Knight, S., Freychet, N., Mineter, M.J., Lehmann, C.E., 2018. Anthropogenic forcings and associated changes in fire risk in Western North America and Australia during 2015/16. *Bull. Am. Meteorol. Soc.* 99 (1), S60–S64.
- Van Wagner, C.E., 1987. Development and Structure of the Canadian Forest Fire Weather Index System. Forestry Technical Report, Canadian Forestry Service Headquarters, Ottawa.
- Vautard, R., van Aalst, M., Boucher, O., Drouin, A., Haustein, K., Kreienkamp, F., Van Oldenborgh, G.J., Otto, F.E., Ribes, A., Robin, Y., Schneider, M., 2020. Human contribution to the record-breaking June and July 2019 heatwaves in Western Europe. *Environ. Res. Lett.* 15 (9), 094077.
- Vitolo, C., Di Giuseppe, F., Barnard, C., Coughlan, R., San-Miguel-Ayanz, J., Libertá, G., Krzeminski, B., 2020. ERA5-based global meteorological wildfire danger maps. *Scientific data* 7 (1), 1–11.
- Voldoire, A., Saint-Martin, D., Sénési, S., Decharme, B., Alias, A., Chevallier, M., Colin, J., Guérémy, J.F., Michou, M., Moine, M.P., Nabat, P., 2019. Evaluation of CMIP6 deck experiments with CNRM-CM6-1. *J. Adv. Model. Earth Syst.* 11 (7), 2177–2213.
- Volodin, E., Gritsun, A., 2018. Simulation of observed climate changes in 1850–2014 with climate model INM-CM5. *Earth Syst. Dynam.* 9 (4), 1235–1242.
- Wang, X., Wotton, B.M., Cantin, A.S., et al., 2017. Cffdrs: an R package for the Canadian forest fire danger rating system. *Ecol. Process.* 6, 5. <https://doi.org/10.1186/s13717-017-0070-z>.
- van der Werf, G.R., Randerson, J.T., Giglio, L., Leeuwen, T.T.V., Chen, Y., Rogers, B.M., Mu, M., Van Marle, M.J., Morton, D.C., Collatz, G.J., Yokelson, R.J., 2017. Global fire emissions estimates during 1997–2016. *Earth Syst. Sci. Data* 9 (2), 697–720.
- van der Wiel, K., Kapnick, S.B., Van Oldenborgh, G.J., Whan, K., Philip, S., Vecchi, G.A., Singh, R.K., Arrighi, J., Cullen, H., 2017. Rapid attribution of the August 2016 flood-inducing extreme precipitation in South Louisiana to climate change. *Hydrol. Earth Syst. Sci.* 21 (2), 897–921.
- World Meteorological Organization, 2021. The Atlas of Mortality and Economic Losses from Weather, Climate and Water Extremes (1970–2019). World Meteorological Organization, Geneva, Switzerland, p. 90.